Selective vibrational excitations in the OX (X = F, Cl, Br, I) molecules

Céline Léonard,[a] Frédéric Le Quéré,[a] Pavel Rosmus,[a] Cristina Puzzarini[b] and Maria Pilar de Lara Castells[b]

[a] *Laboratoire de Chimie Théorique, Université de Marne-la-Vallée, Cité Descartes, 5 Boulevard Descartes, Champs-sur-Marne, F-77454 Marne-la-Vallée, Cedex 2, France*
[b] *Dipartimento di Chimica Fisica ed Inorganica, Università di Bologna, 40136 Bologna, Italy*

Received 12th November 1999, Accepted 26th January 2000

Using *ab initio* calculated potential energy and electric dipole moment functions for the X $^2\Pi$ states of OF, OCl, OBr and OI, two models have been tested to selectively populate their vibrational modes by ultrashort coherent light pulses. For a given form of the pulses either a perturbative approach using discrete vibrational eigenstates and electric dipole transition moment matrix elements or a wavepacket propagation technique were used. The optimisation of the pulse parameters and the mechanisms of the multiphoton processes are discussed. For the target level $v = 10$ populations of more than 60% have been achieved in all four molecules. For OCl it was possible to populate selectively all target levels between $v = 2$ and $v = 15$ using chirped pulses.

1 Introduction

There have been numerous experimental and theoretical studies of the halogen monoxides. The spectroscopic constants of the electronic ground states are well known and extensive calculations have also been performed for the electric dipole moments. We refer to refs. 1–7 for OF, refs. 7–11 for OCl, refs. 6, 7, 12–15 for OBr and refs. 6, 7, 16–19 for OI for previous experimental and theoretical works.

The selective excitations of vibrational modes using femtosecond laser pulses have also been the subject of many theoretical and experimental studies in the past few years (*cf.* for instance refs. 20–22 for theory and refs. 23 and 24 for experiments). In most cases simplified harmonic or anharmonic models have been used to study the mechanism of the multiphoton IR excitations. In the present work such selective vibrational excitations in the electronic ground states of OF, OCl, OBr and OI have been investigated using accurate *ab initio* potential energy and dipole moment functions. The rotation and the fine-structure in the X $^2\Pi$ states were neglected. The aim was to show which selectivity can be achieved with optimal parameters of the pulses and, for O–Cl, how strongly such parameters vary for different vibrational target levels. In the time-dependent computations we used two formalisms. The first is based on the expansion of the time-dependent wavefunctions in the stationary vibrational eigenstates. The second one uses the wavepacket propagation technique. In both cases the same time-dependent model Hamiltonian was employed.

For the OX radicals only the electronic ground states were considered in the optimisation procedure. Similar calculations in which the dissociation *via* the electronically excited state or the ground state (HD^+), and the electronic excitation (OH) were allowed, showed that, with optimised pulses operating in the infrared region and laser intensities between 10^{13}–10^{14} W cm^{-2}, the selective vibrational excitations in the electronic ground states of HD^+ and OH can be the dominating process.

2 Computational methods

For all oxides the electronic structure calculations were performed with complete active space self-consistent field (CASSCF)[25] and internally contracted multireference configuration interaction (MRCI)[26,27] approaches, using as a reference all the configurations, resulting from the full valence CASSCF calculations with the MOLPRO[28] program suite. For OF the spdfg functions of the aug-cc-pVQZ basis set[29] was used. For OCl the spdf subset of the aug-cc-pV5Z was employed for both atoms and was augmented by diffuse s and p functions with the exponents 0.019 16(s), 0.013 92(p) for Cl and 0.0262(s), 0.017 84(p) for O. The same basis set was used for O in OBr, but the bromine basis set was taken from ref. 30. In OI the iodine basis set was taken from ref. 31 and the spdf functions of the aug-cc-pVQZ basis set was employed for O. All dipole moments were calculated from the MRCI energies and finite perturbative method using an external field.

The interaction of the molecule with a polarized electric radiation field in the direction of the molecular axis has been taken into account by the time-dependent perturbation operator in the semiclassical electric dipole approximation, with

$$\boldsymbol{H}(Q, t) = \boldsymbol{H}^0(Q) + \boldsymbol{H}'(Q, t) \quad (1)$$

The operator $\boldsymbol{H}^0(Q)$ corresponds to the radial part of the diatomic nuclear motion Hamiltonian, yielding energies and wavefunctions of discrete states:

$$\boldsymbol{H}^0(Q)\phi_v^0(Q) = E_v^0\,\phi_v^0(Q) \quad (2)$$

The perturbation operator $\boldsymbol{H}'(Q, t)$ has the form

$$\boldsymbol{H}'(Q, t) = -\mu(Q)A(t). \quad (3)$$

In this equation $\mu(Q)$ is the dipole moment function and $A(t)$ the analytic form of the pulse.

We were interested in the probabilities $P_v(t)$ of finding the molecule in the v-th eigenstate, which were calculated by the

projection of $\Phi(Q, t)$, the time-dependent wavefunction, on the vibrational eigenstate $\phi_v^0(Q)$:

$$c_v(t) = \langle \Phi(Q, t) | \phi_v^0(Q) \rangle \quad (4)$$

$$P_v(t) = |c_v(t)|^2 \quad (5)$$

Two kinds of pulses were studied: the first one with ω independent of time

$$A(t) = \cos(\omega t)\varepsilon(t) \quad (6)$$

and the second one with a time dependent "chirped" ω in the IR range.

$$A'(t) = \cos[\omega(t)t]\varepsilon(t) \quad (7)$$

with

$$\omega(t) = \omega_2 + (\omega_1 - \omega_2)\exp[-(t/\tau)^2] \quad (8)$$

where ω_1 is the initial wavenumber, ω_2 the asymptotic wavenumber, τ describes the switching between ω_1 and ω_2 and $\varepsilon(t)$ is the shape function which modulates the pulse in time.

Both pulses have a $\sin^2$ shape function given by,

$$\varepsilon(t) = E_0 \sin^2(\pi t/t_p)$$

$$\text{for} \quad 0 \leqslant t \leqslant t_p, \ \varepsilon(t) = 0 \quad \text{if} \quad t > t_p \quad (9)$$

where t_p is the pulse duration, and E_0 is the field strength.

Such pulse forms were recommended, for instance, by Jakubetz *et al.*[20] in order to achieve high vibrational selectivity. The non-chirped pulse depends on three parameters, ω, t_p and E_0, and the chirped pulse on five parameters ω_1, ω_2, E_0, τ and t_p. We have optimized these parameters for selected target state always starting from $v = 0$. The pulse duration, t_p, has been set to 1 ps in most of the calculations. All other parameters were optimised simultaneously using a downhill simplex method,[32] and the discrete state representation.

The radial Schrödinger equation for nuclear motion was solved by the Numerov method.[33] In the discrete state representation, the time-dependent wavefunction is expanded in the basis of the vibrational eigenstates, neglecting the dissociative continuum:

$$\Phi(Q, t) = \sum_v c_v(t)\phi_v^0(Q, t) \quad (10)$$

$$\phi_v^0(Q, t) = \phi_v^0(Q)e^{-iE_v^0 t} \quad (11)$$

The time-dependent problem consists of the coupled set of differential equations:

$$i\dot{c}(t) = \boldsymbol{H}c(t) \quad (12)$$

which was solved by a standard Runge–Kutta numerical method.[34]

The number of bound vibrational wavefunctions used in expansion (9) was 23 for OF, 34 for OCl, 33 for OBr and 29 for OI.

The time propagation of the wavepacket was performed using a short iterative Lanczos method.[35] In contrast with the previous method, the propagation of the wavepacket does not involve explicit calculations of the vibrational states. These states were computed independently in order to obtain the population probabilities [*cf.* eqns. (4) and (5)]. The wavepacket propagation technique gives the same results as the discrete state representation approach for the oxides, but it was more appropriate to use this approach in the case of the dissociation of HD^+ (*cf.* section 3).

3 Results

In Table 1 the spectroscopic constants calculated in the present work are compared with previous experimental and theoretical data for the electronic ground states of OF, OCl, OBr and OI. The equilibrium distances agree with experiment to within 0.001 Å (OF) to 0.01 Å (OCl), the largest deviation of the harmonic wavenumber amounts to 13 cm^{-1} (OI). The electric dipole moments in the vibrational ground states are calculated with an accuracy better than 0.05 D in all cases,† and also the 1–0 transition moment for all four oxides agrees very well with the available experimental data. In Table 2 the analytic expansions of the calculated dipole moment functions are given. Fig. 1 shows the calculated potential energy functions with the corresponding vibrational energy levels used in the present calculations and the dipole moment functions. All four dipole moment functions have extrema in the region of the classical turning points of moderately excited vibrational levels. Only the dipole moment function of OF changes its sign close to the equilibrium distance, in this region its slope is steeper than for OCl, OBr and OI. Nevertheless, if high vibrational levels are involved in the pumping process the function can not be approximated only by its first derivative at R_e (*cf.* Table 2 for comparison of the expansion coefficients in all four oxides). The transition moments for the $\Delta v = 1$, 2, 3 transitions are displayed in Fig 2. For OCl, OBr and OI, the transition moments $\Delta v = 1$ are small between the low lying vibrational levels and increase linearly with v. The $\Delta v = 1$ transition moments in OF are distinctly larger and reach a maximum for $v = 8$.

Before studying the mode selective excitations in the oxides, we have tested the present approach against the results obtained for the dissociation of HD^+ by Charron *et al.*[36] This process involves the ground and the first repulsive electronic states. The input data were taken from their work. The initial level in the calculations of Charron *et al.* was arbitrarily chosen to be $v = 3$ in the electronic ground state of HD^+. With the pulse parameters of ref. 36 and our wavepacket approach we could almost exactly reproduce their results for the dissociation probabilities. We found, however, that it is possible to dissociate HD^+ even if the initial level is the vibrational ground state with longer pulse duration. For instance, for a 1 ps chirped pulse with $\omega_1 = 3113$ cm^{-1}, $\omega_2 = 1995$ cm^{-1}, $\tau = 94.9$ fs and $E_0 = 0.037\,742$ E_h/ea_0 the molecule dissociates with a probability of 31.2%. With a non-chirped 1 ps pulse with $\omega = 1600$ cm^{-1}, $E_0 = 0.037\,742$ E_h/ea_0 the probability increases to 51%. In Fig. 3 it is shown that a non-chirped pulse is able to dissociate HD^+ rather efficiently starting from $v = 0$ within 1 ps and with ω's between 1400 and 1900 cm^{-1}. For shorter pulses with $t_p = 200$ fs, $\omega = 1910$ cm^{-1}, and $E_0 = 0.037\,74$ E_h/ea_0 we could, for instance, populate to 66% the $v = 3$ level of the ground state, and the dissociation represented only a marginal fraction of the overall process. In similar computations with very accurate potential energy, dipole and transition moments for the X and A state of the OH radical (ref. 37) we were able to populate completely, for instance, the $v = 4$ level of the X state with the following parameters: $E_0 = 0.0917$ E_h/ea_0, $\omega = 3333$ cm^{-1} and $t_p = 1586$ fs. Other sets of pulse parameters can populate the A state vibrational levels to 100%.[37] These two model examples show that the pulse parameters can be optimised in such a way that mainly the vibrational levels of the electronic ground states are populated even with high laser intensities.

In Table 3 it is shown that in all oxides the arbitrary chosen $v = 10$ level can be selectively populated with both non-chirped and chirped pulses with the optimised pulse parameters given in the table. With the nonchirped pulse the selectivity decreases from OF to OI. The chirped pulses are much more efficient since the $v = 10$ level is populated even in OI to more than 70%. For OI the optimised electric field is twice as intense as in the other diatomics and the $\Delta v = 2$ tran-

† 1 D (debye) ≈ $3.335\,64 \times 10^{-30}$ C m.

Table 1 Spectroscopic constants

	R_e/Å	B_e/cm^{-1}	α_e/cm^{-1}	ω_e/cm^{-1}	$\omega_e x_e$/cm^{-1}	μ_0/D	μ_{01}/D
OF							
This work	1.355	1.0567	0.0137	1047.1	10.4	−0.0283	−0.1042
Exp.[1]	1.354						
Exp.[2]		1.0587	−0.0133	1053.0	−9.9		
Exp.[3] [a]						−0.0043	
Calc.[7]	1.356	1.056	0.0206	1026.7	22.3	−0.012	−0.099
Calc.[5]						−0.0089	
OCl							
This work	1.579	0.6163	0.0053	852.3	4.9	1.2537	−0.0346
Exp.[8] [a]						1.2974	−0.034
Exp.[9]	1.56960	0.6235	0.0059				
Exp.[10]		0.6235	0.0059	853.8	5.6		
Calc.[7]	1.578	0.6171	0.0056	854.3	4.9	1.278	−0.035
OBr							
This work	1.726	0.4257	0.0034	728.5	3.5	1.7110	−0.0268
Exp.[12]						1.765	
Exp.[13] [a]	1.721	0.4281	0.003 64	727.0	4.7		
Exp.[14] [a]							−0.0252
Calc.[7]	1.729	0.4242	0.0032	728.0	2.6	1.711	−0.025
OI							
This work	1.879	0.3362	0.0027	694.5	4.6	2.4487	−0.0012
Exp.[16]						2.45[c]	
Exp.[17] [a]	1.867	0.3402	0.0027	681.6	4.4		
Exp.[18] [b]	1.887			658.0	4.4		
Calc.[7]	1.899	0.3290	0.0024	670.5	2.9	2.303	−0.008

[a] For the X $^2\Pi_{3/2}$ component. [b] For the X $^2\Pi_{1/2}$ component. [c] Equilibrium value of the dipole moment function.

sitions are strongly involved (*cf.* Fig. 2). Since the density of states is also larger the optimum τ becomes larger than in the other oxides. In Fig. 4 the Fourier transform of the chirped pulse optimised for $v = 10$ of OCl (*cf.* Table 3) is shown. The largest pulse intensity is situated between the wavenumbers for the $\Delta v = 1$ transitions 1–0(v_i) and 10–9(v_f). At this stage of the process many vibrational levels are involved in order to reach highly excited vibrational states. The ω_1 and ω_2 wavenumbers of the optimised chirped pulse are shifted to higher energies by comparison with the initial and final $\Delta v = 1$ energy differences, which were used as a starting point in the optimisation procedure for the ω's. If τ equals t_p (the duration of the pulse) the maximum is situated between ω_1 and ω_2. The optimum pulse, however, requires much shorter τ's, which results in a shift of the maximum towards smaller wavenumbers. This is necessary in order to change rapidly the populations of the involved vibrational states during the period with maximum intensity of the pulse.

In Fig 5 we have plotted the populations in the lowest 22 vibrational levels of the four oxides for the optimised chirped pulses from Table 3. The dotted lines show relative populations of the initial $v = 0$ and the final target level $v = 10$. The solid lines represent populations of other levels in the process lasting 1 ps. In each case we observed a significant population of levels above the target state. This trend is understandable

Table 2 Coefficients (in au) of the polynomial expansion about the equilibrium geometry[a] of the dipole moment functions for OF, OCl, OBr and OI up to fourth-order

	μ_e	C_1	C_2	C_3	C_4
OF	−0.0091	−0.5143	0.3415	0.1711	−0.1481
OCl	0.4961	−0.1475	−0.3952	0.3716	−0.1784
OBr	0.6772	−0.1147	−0.3668	0.2357	−0.0674
OI	0.9674	0.014 72	−0.4438	0.1534	0.013 31

[a] $\mu(R) = \mu_e + C_1(R-R_e) + C_2(R-R_e)^2 + C_3(R-R_e)^3 + C_4(R-R_e)^4$.

Table 3 Optimisation results for OF, OCl, OBr and OI for the population of the $v = 10$ level with $t_p = 1$ ps

	Non-chirped pulse		
	E_0^a /(E_h/ea_0)	ω_{opt}/cm^{-1}	Population
OF	0.029	920.4	0.669
OCl	0.030	801.9	0.533
OBr	0.034	693.9	0.501
OI	0.076	1289.2	0.358

	Chirped pulse				
	E_0 [a]/(E_h/ea_0)	ω_1/cm^{-1}	ω_2/cm^{-1}	τ/fs	Population
OF	0.031	959.1	926.4	252.5	0.844
OCl	0.039	918.0	813.0	236.3	0.833
OBr	0.046	818.3	705.0	236.3	0.796
OI	0.097	1366.5	1303.2	326.6	0.716

[a] Relation between the intensity and the electric field strength: $I[W/cm^2] = 3.511\,29 \times 10^{16}\, E_0^2\, (E_h/ea_0)$.

Table 4 Optimisation results for OCl with chirped pulses and $t_p = 1$ ps for the population of the $v = 2$–15 vibrational levels

Vibrational levels	$E_0/E_h/ea_0$	ω_1/cm^{-1}	ω_2/cm^{-1}	τ/fs	Population
2	0.024	1064.6	868.2	161.6	0.579
3	0.025	1041.6	861.5	177.3	0.592
4	0.025	1006.8	855.7	199.8	0.636
5	0.026	996.5	849.0	208.8	0.686
6	0.027	979.6	842.1	218.3	0.729
7	0.030	963.6	835.1	225.7	0.766
8	0.033	949.2	828.0	230.4	0.796
9	0.036	934.0	820.7	234.0	0.819
10	0.039	918.0	813.0	236.3	0.833
11	0.043	901.1	805.2	237.6	0.838
12	0.047	883.1	797.0	237.8	0.831
13	0.052	864.9	788.6	236.8	0.815
14	0.056	848.0	780.1	234.6	0.783
15	0.061	823.9	772.1	242.9	0.747

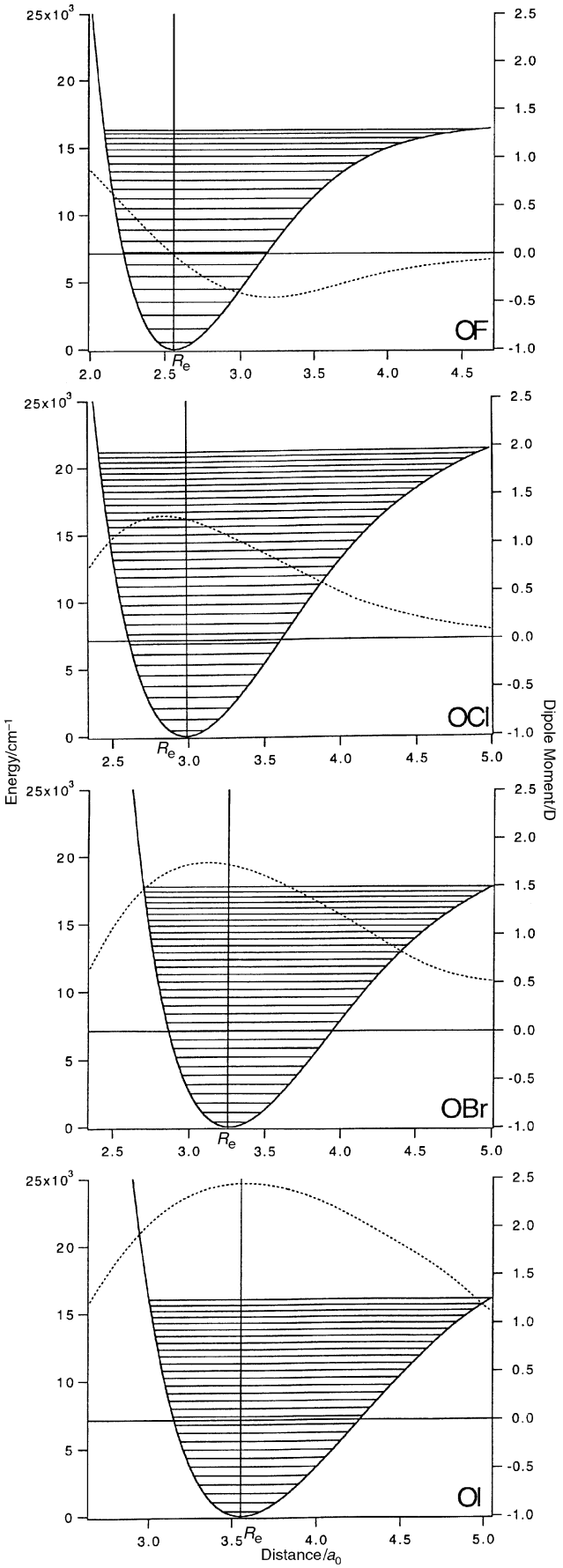

Fig. 1 Potential energy, dipole moment functions and the vibrational energy levels of OF, OBr, OCl and OI.

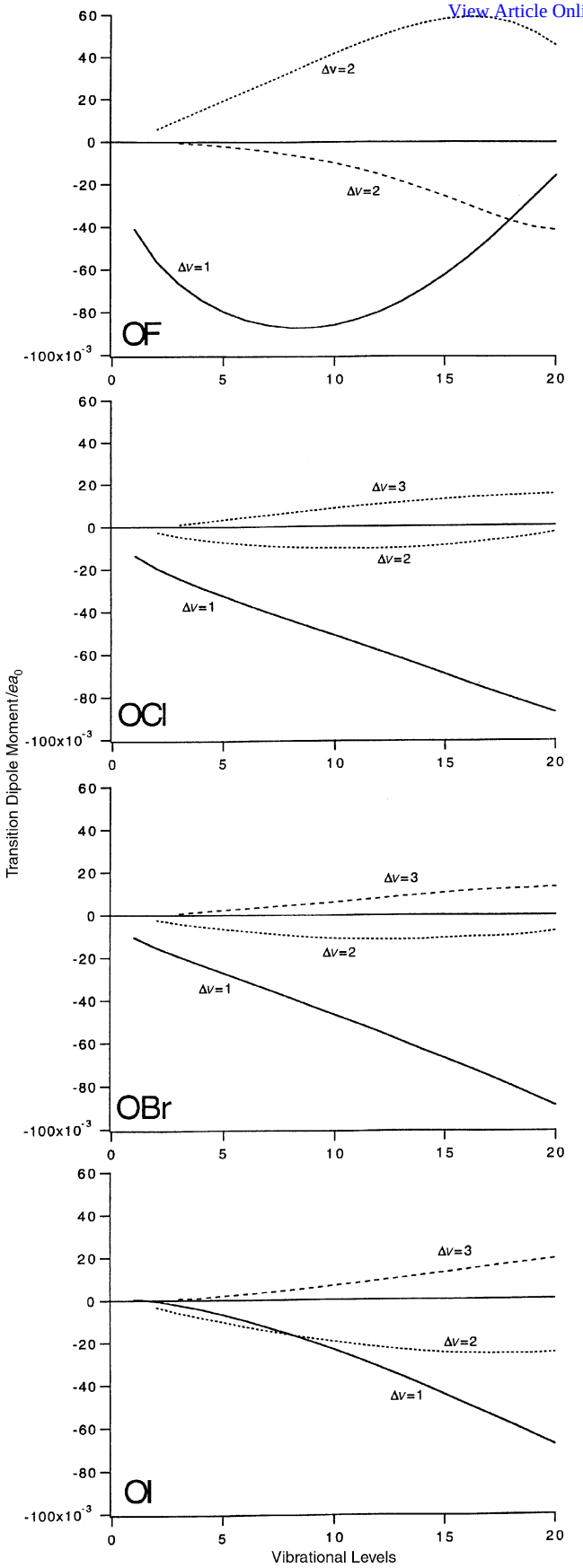

Fig. 2 Transition dipole moments matrix elements for $\Delta v = 1, 2, 3$ of OF, OBr, OCl and OI (in ea_0).

from the larger bandwidth of the pulse (*cf.* Fig. 4). As described by Jakubetz *et al.*,[20] the first third of the pulse duration leads mainly to the depopulation of $v = 0$, the second to the step by step population of the higher vibrational levels during the maximum intensity range of the pulse and the last one the selective population of the target state. The pulses

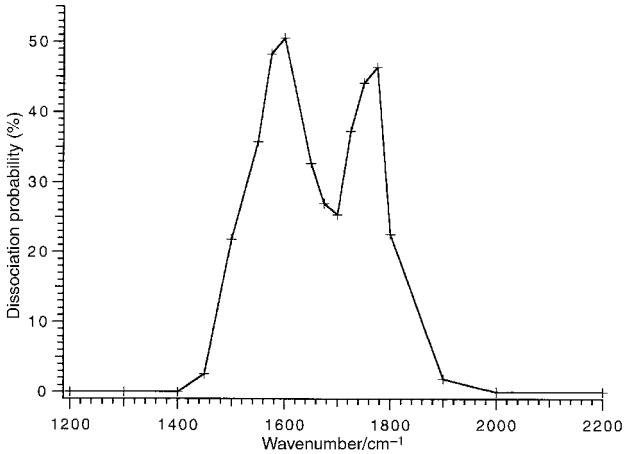

Fig. 3 Dissociation probability of HD^+ plotted against the wavenumbers for a non-chirped pulse with $t_p = 1$ ps and $E_0 = 0.037\,742\ E_h/ea_0$ (*cf.* text).

show a direct path through $\Delta v = \pm 1$ transitions to reach the target state (*cf.* Fig. 5) from $v = 0$ to $v = 10$ with $\Delta v = +1$ ($+2$ for OI). The non-direct path involves excited states above the target state. They are populated at the beginning of the decreasing part of the pulse shape giving them a quite large population around $0.8t_p$.

In Table 4 we have chosen the OCl molecule as an example for selective population of various target states $v = 2$ to $v = 15$ using chirped pulses. In all cases we have obtained selective populations between about 60 to 80%. With increasing vibrational quantum numbers the electric field increases, whereas ω_1 and ω_2 decrease because lower wavenumbers are needed in the maximum intensity range of the pulse to populate higher vibrational levels. Since the energy difference between the vibrational levels decreases with v, τ increases with v. With the parameters in Table 4, 1 ps is an appropriate time to populate mainly the levels lying close to $v = 11$.

4 Conclusions

The halogen oxides are of particular interest for atmospheric chemistry, and studies of their reactivity in selectively excited vibrational states would considerably contribute to a better understanding of their reaction dynamics.

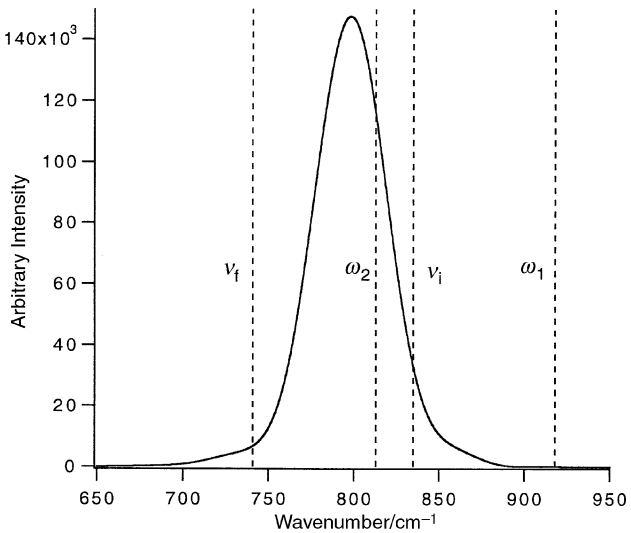

Fig. 4 Fourier transform (in arbitrary units) of the chirped pulse ($\omega_1 = 918.0$ cm^{-1}, $\omega_2 = 813.0$ cm^{-1}, $E_0 = 0.039\ E_h/ea_0$, $\tau = 236.3$ fs and $t_p = 1$ ps) which was used to populate selectively the $v = 10$ level of OCl. ν_i and ν_f are respectively the wavenumbers for the transitions 1–0 and 10–9.

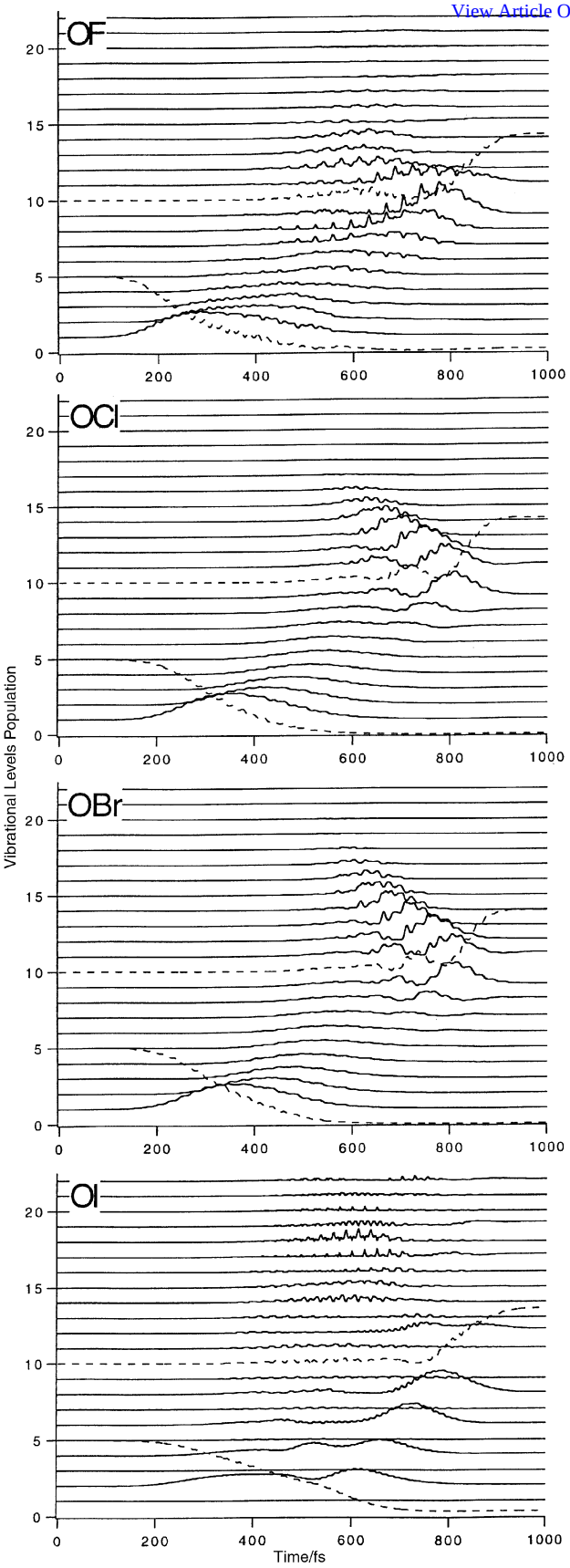

Fig. 5 The time evolution of the populations of the vibrational states for the target state $v = 10$ for OF, OCl, OBr and OI with chirped pulses (*cf.* Table 3 for parameters). Only the relative changes of the populations are shown.

The present model study using high quality *ab initio* potential and electric dipole moment functions shows that selective vibrational populations in OX electronic ground states can be achieved particularly with chirped pulses. For 1 ps pulses the

parameters have been optimised numerically. It is shown that selective populations of highly excited vibrational states will require very fine tuning of the pulse parameters. For instance, in OCl only 5% of the intensity and 2% of the ω_1 and ω_2 values make the difference between the dominating populations of the $v = 10$ and 11 levels. High selectivity in systems with larger density of vibrational states and decreasing radiative transition probabilities (OI) can be achieved only with much stronger electric fields. The results presented in Tables 3 and 4 show that the optimised parameters depend in a very complex way on the energies of the vibrational levels and the transition dipole matrix elements.

Acknowledgements

Financial support from the EEC as part of the TMR network Potential Energy Surfaces for Spectroscopy and Dynamics, contract No. FMRXCT96-088(DG12-BIUO) is gratefully acknowledged.

References

1 J. B. Burkholder, P. D. Hammer, C. J. Howard and A. R. W. McKellar, *J. Mol. Spectrosc.*, 1986, **118**, 471.
2 P. D. Hammer, A. Sinha, J. B. Burkholder and C. J. Howard, *J. Mol. Spectrosc.*, 1988, **129**, 99.
3 A. R. W. McKellar, *J. Mol. Spectrosc.*, 1983, **101**, 186.
4 M. W. Chase, *J. Phys. Chem. Ref. Data*, 1996, **25**, 551.
5 S. R. Langhoff, C. W. Bauschlicher Jr. and H. Partridge, *Chem. Phys. Lett.*, 1983, **102**, 292.
6 Z. Zang, P. S. Monks, L. J. Stief, J. F. Liebman, R. E. Huie, S.-C. Kuo and R. B. Klemm, *J. Phys. Chem.*, 1996, **100**, 63.
7 M. P. McGrath and F. S. Rowland, *J. Phys. Chem.*, 1996, **100**, 4815.
8 D. Yaron, K. Peterson and W. Klemperer, *J. Chem. Phys.*, 1988, **88**, 4702.
9 J. A. Coxon, *Can. J. Phys.*, 1979, **57**, 1538.
10 A. G. Maki, F. J. Lovas and W. B. Olson, *J. Mol. Spectrosc.*, 1982, **92**, 410.
11 L. G. M. Pettersson, S. R. Langhoff and D. P. Chong, *J. Phys. Chem.*, 1986, **85**, 2836.
12 K. P. Hubert and G. Herzberg, *Constants of Diatomic Molecules*, Van Nostrand, New York, 1979.
13 J. E. Butler, K. Kawaguchi and E. Hirota, *J. Mol. Spectrosc.*, 1984, **104**, 372.
14 J. J. Orlando, J. B. Burkholder, A. M. R. P. Bopegedera and C. J. Howard, *J. Mol. Spectrosc.*, 1991, **145**, 278.
15 M. W. Chase, *J. Phys. Chem. Ref. Data*, 1996, **25**, 1069.
16 C. R. Byfleet, A. Carrington and D. K. Russell, *Mol. Phys.*, 1971, **20**, 271.
17 J. P. Bekooy, W. L. Meerts and A. Dymanus, *J. Mol. Spectrosc.*, 1983, **102**, 320.
18 M. K. Gilles, M. L. Polak and W. C. Lineberger, *J. Chem. Phys.*, 1991, **95**, 4723.
19 M. W. Chase, *J. Phys. Chem. Ref. Data*, 1996, **25**, 1297.
20 W. Jakubetz, B. Just, J. Manz and H.-J. Schreier, *J. Phys. Chem.*, 1990, **94**, 2294.
21 Y. Chen, P. Gross, V. Ramakrishna, H. Rabitz and K. Mease, *Chem. Phys. Lett.*, 1996, **252**, 447.
22 B. Just, J. Manz and I. Trisca, *Chem. Phys. Lett.*, 1992, **193**, 423.
23 N. Bloembergen and A. H. Zewail, *J. Phys. Chem.*, 1984, **88**, 5459.
24 K. B. Moller and A. H. Zewail, *Chem. Phys. Lett.*, 1998, **295**, 1.
25 P. J. Knowles and H. J. Werner, *Chem. Phys. Lett.*, 1985, **115**, 259.
26 P. J. Knowles and H. J. Werner, *J. Chem. Phys.*, 1988, **89**, 5803.
27 P. J. Knowles and H. J. Werner, *Chem. Phys. Lett.*, 1988, **145**, 514.
28 MOLPRO is a package of ab initio programs written by H. J. Werner and P. J. Knowles, with contributions by R. D. Amos, A. Berning, D. L. Cooper, M. J. O. Deegan, A. J. Dobbyn, F. Eckert, C. Hampel, T. Leininger, R. Lindh, A. W. Lloyd, W. Meyer, M. E. Mura, A. Nicklass, P. Palmieri, K. Peterson, R. Pitzer, P. Pulay, G. Rauhut, M. Schuetz, H. Stoll, A. J. Stone and T. Thorsteinsson. Further details at www.tc.bham.ac.uk/molpro.
29 (*a*) T. H. Dunning, *J. Chem. Phys.*, 1989, **90**, 1007; (*b*) D. E. Woon and T. H. Dunning and Jr., *J. Chem. Phys.*, 1993, **98**, 1358.
30 P. Palmieri, C. Puzzarini and R. Tarroni, *Chem. Phys. Lett.*, 1981, **256**, 409.
31 P. Rosmus, H.-J. Werner and E.-A. Reinsch, *Chem. Phys. Lett.*, 1981, **78**, 311.
32 J. A. Nelder and R. Mead, *Comput. J.*, 1965, **7**, 308.
33 J. W. Cooley, *Math. Comput.*, 1961, **15**, 363.
34 J. Stoer and R. Burlisch, *Introduction to Numerical Analysis*, Springer-Verlag, New York, 1980.
35 T. J. Park and J. C. Light, *J. Chem. Phys.*, 1986, **85**, 5870; J. K. Cullum and R. A. Willoughby, *Lanczos Algorithms for Large Symmetric Eigenvalue Computation*, Birkaüser, Boston, 1985.
36 E. Charron, A. Giusti-Suzor and F. H. Meis, *J. Chem. Phys.*, 1995, **103**, 7359; E. Charron, *Contrôle cohérent de la photodissociation en champ laser intense*, Université de Paris-Sud, France, 1994.
37 M. P. de Lara Castells, A. Mitrushenkov, P. Palmieri, F. Le Quéré, C. Léonard and P. Rosmus, *Mol. Phys.*, submitted.

Paper a908993d